JGR Atmospheres

REVIEW ARTICLE
10.1029/2018JD029830

Key Points:
- A decade of research on the meteorology of Heron Reef in the Great Barrier Reef, Australia, is reviewed
- Energy flux and trace gas exchange with the atmosphere over Heron Reef under a range of conditions including coral bleaching are summarized
- Suggestions are made for future research to advance understanding of coral reef – atmosphere interactions

Correspondence to:
H. McGowan,
h.mcgowan@uq.edu.au

Citation:
McGowan, H., Sturman, A., Saunders, M., Theobald, A., & Wiebe, A. (2019). Insights from a decade of research on coral reef—Atmosphere energetics. *Journal of Geophysical Research: Atmospheres*, *124*, 4269–4282. https://doi.org/10.1029/2018JD029830

Received 13 OCT 2018
Accepted 15 MAR 2019
Accepted article online 8 APR 2019
Published online 29 APR 2019

Author Contributions:
Conceptualization: Hamish McGowan
Formal analysis: Hamish McGowan, Melissa Saunders, Alison Theobald, Andrew Wiebe
Investigation: Hamish McGowan, Melissa Saunders, Alison Theobald, Andrew Wiebe
Methodology: Hamish McGowan, Andrew Sturman, Melissa Saunders, Alison Theobald, Andrew Wiebe
Project administration: Hamish McGowan, Andrew Sturman
Resources: Hamish McGowan, Andrew Sturman
Writing - original draft: Hamish McGowan
Writing – review & editing: Andrew Sturman

Insights From a Decade of Research on Coral Reef—Atmosphere Energetics

Hamish McGowan[1], Andrew Sturman[2], Melissa Saunders[1], Alison Theobald[3], and Andrew Wiebe[4]

[1]Atmospheric Observations Research Group, School of Earth and Environmental Sciences, University of Queensland, Brisbane, Queensland, Australia, [2]Department of Geography, University of Canterbury, Christchurch, New Zealand, [3]Department of Environment and Science, Queensland Government, Brisbane, Queensland, Australia, [4]Weather Climate Insight, Kelowna, British Columbia, Canada

Abstract Coral reefs cover approximately 0.10 to 0.25% of the marine environment and yet are home to around 25% of marine species and support the livelihoods of more than 500 million people. They face a wide range of threats, with the impact of global warming gaining most attention due to its frequently claimed causal link to coral bleaching. Here we review a decade of research into the micrometeorology of Heron Reef, a lagoonal platform coral reef in the southern Great Barrier Reef, Australia. Using novel pontoon-mounted eddy covariance systems, we show that often >80% of net radiation is partitioned into heating the water overlying the reef, the reef benthos, and substrate. Significant spatial variability in energy and trace gas exchanges occurs over the reef in response to different geomorphic and hydrodynamic conditions. Synoptic weather patterns that bring light winds, clear skies, and high humidity, result in reef scale meteorology that appears to have a greater influence on coral bleaching events than the background oceanic warming trend. The reef develops its own convective internal boundary layer, with potential to influence cloud development and therefore the surface energy balance. Knowledge of such local effects is lacking, so it is recommended that future research is needed into reef scale processes and how they interact with larger-scale forcing.

1. Introduction

Understanding energy and trace gas exchanges between the Earth's surface and atmosphere is fundamental to correct attribution of meteorological processes and accurate prediction of weather and climate. Modeling impacts of anthropogenic changes to surface properties, atmospheric trace gases and turbidity is dependent on direct measurements of the surface-atmosphere energy and trace gas exchanges that underpin model initialization and validation. Global monitoring of energy and trace gas exchanges between the Earth's surface and the overlying atmosphere has been established under the theme of FLUXNET (Baldocchi et al., 2001) with national programs including AmeriFlux (Hollinger et al., 1999), AsiaFlux (Tani et al., 2008), OzFlux (Beringer et al., 2016), EUROFLUX (Tenhunen et al., 1998), and ChinaFLUX (Yu et al., 2006). These programs focus on terrestrial energy balance monitoring and primarily CO_2 exchanges between the surface and atmosphere using the eddy covariance method. Far fewer measurements have been made over the oceans, with these typically confined to short case study periods using research vessels as measurement platforms (Butterworth & Miller, 2016; McGillis et al., 2004). The additional complexity and cost of undertaking direct measurements of energy and trace gas exchanges from ships or buoys means that such data are rare, none more so than over coral reefs.

Coral reefs cover 2.8 to 6.0 × 10^5 km^2 of the Earth's tropical and subtropical oceans (~0.1% to 0.25% of the marine environment) and yet are home to around 25% of marine species and support the livelihoods of more than 500 million people (Frieler et al., 2013; Hoegh-Guldberg et al., 2007). Often referred to as "rainforests" of the oceans, coral reefs face a wide range of threats from overfishing, mining, pollution, coastal development, invasive species, and inadequately managed tourism. However, it has been global warming and its correlation with more frequent coral bleaching events over the past 25 years, often concurrent with El Niño-Southern Oscillation (ENSO) events, which has gained most attention (Claar et al., 2018; Pandolfi et al., 2011).

Coral bleaching occurs when environmental stressors, in this case warm waters exceeding the thermal tolerance of corals, cause a breakdown of the coral-algae symbiosis with the algae expelled from the coral,

leading to the emergence of the white coral skeleton (bleaching; see Brown, 1997). Coral bleaching may also be triggered by unusually cold water temperatures and/or combinations of other factors that stress corals. Thus, while much has been made of the correlation between more frequent coral bleaching events and rising global temperatures, direct measurements of energy exchanges over coral reefs that give rise to changes in their thermal environment have been rare.

1.1. Previous Research

The main energy and trace gas exchanges that occur over coral reefs are shown in Figure 1, including CO_2. While coral reefs are known to emit dimethyl sulfide (DMS; and numerous other volatile organic compounds), which may influence cloud microphysical processes, these are not considered further here and readers are directed to, for example, Swan et al. (2016), and references therein.

The surface energy balance of a coral reef can be written as

$$Q^* = Q_e + Q_h + \Delta Q_s + \Delta Q_a + Q_r + Q_g \quad (1)$$

where Q^* is net all wave radiation; Q_e, latent heat flux; Q_h, sensible heat flux; ΔQ_s, change in heat storage of the layer of water overlying the coral reef; ΔQ_a, net horizontal advection of heat in the water overlying the reef by currents; Q_r, addition or loss of heat associated with rainfall; and Q_g, heat transfer via conduction and radiation transfers into or out of the reef substrate (McGowan et al., 2010).

In the absence of rainfall, or where periods of rainfall have been excluded from the data, for example, because of their impact on open path gas analysers and sonic anemometers, Q_r can be removed and ΔQ_a and Q_g combined with ΔQ_s. This is permissible due to existing uncertainties associated with accurate measurement of advection of heat in currents over a coral reef and conduction into the structurally complex benthos and reef substrate. Accordingly, equation (1) can be simplified to

$$Q^* = Q_e + Q_h + \Delta Q_{swr} \quad (2)$$

where, ΔQ_{swr} is the change in heat storage of the layer of water overlying the coral reef, the benthos and the reef substrate (McGowan et al., 2010).

Direct measurements of these energy fluxes have typically been made during onshore winds using meteorological towers located on shorelines adjacent to coral reefs or from towers built on reef flats (Davis et al., 2011; Garratt & Hyson, 1975; Kjerfve, 1978; Smith, 2001). Vertical fluxes of momentum, Q_h and Q_e downwind of a coral reef during a winter cold-air outbreak in the South China Sea were measured by Garratt and Hyson (1975). Latent heat flux and Q_h peaked at 550 and 110 W/m^2, respectively, highlighting the effect of wind speed and air-reef-water temperature differences as principal controls of the turbulent flux exchanges with the atmosphere. Kjerfve (1978) made observations in Belize over a 2-week period in June 1975 and found Q_e to be the dominant energy exchange over a shallow reef flat, with a daily mean flux of 202 W/m^2 equating to about 4 times the magnitude of Q_h. Smith (2001) calculated Q_h and Q_e at Lee Stocking Island over shallow reef water in the Bahamas during July and August from standard meteorological and hydrological data. He found Q_h to range from −35 W/m^2 to +35 W/m^2 with Q_e from 35 to 130 W/m^2. McCabe et al. (2010) used a bulk formula approach to estimate Q_e and Q_h over the reef flat at Lady Elliot Island in the southern Great Barrier Reef, Australia, during the Austral autumn. They found that evaporative cooling induced by increased wind speeds was the dominant heat sink with increases in Q_e of up to 60% (250 W/m^2) associated with wind speeds increasing from 3 to 4 m/s to 10 to 12 m/s.

While these rare studies over the past 50 years have enabled greater insight into energy and trace gas exchanges over coral reefs, significant gaps remain in understanding the controls on these processes and their relationship to prevailing synoptic meteorology and the biophysical attributes of coral reefs. This stands in stark contrast to the plethora of research on surface energy balances over terrestrial surfaces including rainforests, snow and ice, crops, and urban landscapes. Furthermore, no studies have previously made direct measurements of carbon exchange with the atmosphere over coral reefs at fine spatiotemporal scales (>10^2 m^2 and minutes to days) to shed light on whole-of-reef CO_2 exchange with the atmosphere (McGowan et al., 2016). Again, this highlights the lack of knowledge of coral reefs and their interactions with the atmosphere

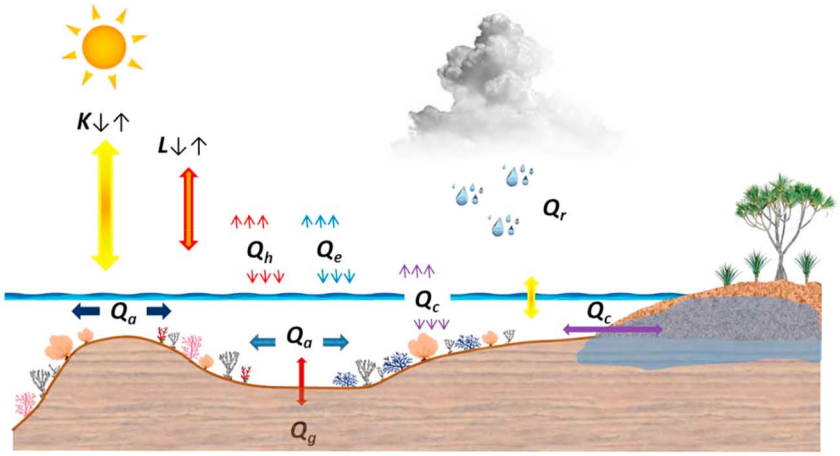

Figure 1. Schematic diagram showing the main energy and trace gas fluxes over a coral reef with arrows indicating direction of movement. Q_a is advection of heat associated with currents between the ocean and reef (dark blue arrows) and across the reef (light blue arrows); Q_c is CO_2 exchanges including that with ground water drainage through carbonate sands onto the reef; Q_g is ground heat flux into/from the reef benthos and substrate; Q_r is heat flux associated with rain; Q_h sensible heat; Q_e latent heat; K solar shortwave radiation including reflected from the water surface and coral sand on reef flats; L is longwave radiation from the water surface and atmospheric water vapor including clouds and trace gases such as CO_2. Not shown is Q^*(net radiation) and ΔQ_s (change in storage).

at a time when many consider their very existence to be threatened by development, invasion by exotic pests, over fishing and global warming.

Here we review a decade of research into energy and trace gas exchanges between the reef and overlying atmosphere on the southern Great Barrier Reef, Australia. The primary aim of this research program was to quantify controls on the thermal environment of the reef under a range of weather conditions using the eddy covariance method to better inform the debate on coral bleaching and the role of coral reefs in the global carbon budget.

2. Field Area

Our research focused on Heron Reef, a typical lagoonal platform reef located on the southern Great Barrier Reef (GBR) 80 km northeast of Gladstone on the northeast coast of Australia (Figure 2). As described in McGowan et al. (2010), MacKellar, McGowan, and Phinn (2012), and MacKellar, McGowan, Phinn, and Soderholm (2012), Heron Reef covers ~27 km^2, having developed on an antecedent karst platform with episodes of growth corresponding with higher sea levels during Holocene sea level fluctuations (Hopley et al., 2007). The reef extends southeastward from Heron Island, which is located on the northwest margin of the reef. The island itself is ~800-m long and 280-m wide and is one of over 300 coral cays on the GBR, the world's largest emergent reef system covering ~345,950 km^2 and consisting of more than 2,900 coral reefs (Woodroffe, 2003).

Annual rainfall at Heron Reef is ~1,050 mm, with the majority of precipitation occurring during summer (December to February) and in autumn (March to May). June to September is the driest period of the year when anticyclones track east across the Australian continent and bring mostly calm and settled conditions to the area. The wind regime of Heron Reef is dominated by the southeasterly trade winds, while a more westerly component develops during winter following the passage of cold fronts over southern Australia. Wind direction becomes more variable in summer with the occurrence of occasional strong northeasterlies, although southeasterly winds still dominate. The strongest winds are associated with the passage of tropical cyclones during the summer. The highest mean daily maximum air temperature occurs in January at 29.8 °C, with the lowest mean daily minimum air temperature occurring in July at 16.7 °C (MacKellar, McGowan, & Phinn, 2012; MacKellar, McGowan, Phinn, & Soderholm, 2012; McGowan et al., 2010).

Fortuitously, to enable our research to reflect the physical properties of Heron Reef, previous work has classified the reef into geomorphic zones with distinctive hydrodynamic and geomorphic characteristics, as well as benthic assemblages (Jell & Flood, 1978; Phinn et al., 2011). The reef flat, shallow, and deep lagoon sites

Figure 2. Location map and satellite image of Heron Reef with eddy covariance measurement sites indicated. Satellite image of Heron Reef was obtained from the Ikonos satellite and provided by DigitalGlobe and the Centre for Spatial Environmental Research.

on Heron Reef, respectively, cover 32% [sand (21%), algae (28%), rubble and sand (48%), benthic microalgae (1.8%), live coral (0.2%)], 16% [sand (52%), coral bommies (2.5%), rubble (0.5%), benthic microalgae (45%)], and 12% [coral bommies (21%), sand (79%)] of the total reef surface. The remaining area of Heron Reef is composed of the outer reef flat, reef slope, reef crest, and the coral cay, which cover 20%, 13%, 6%, and 1%, respectively. The coral *Acropora* spp. is prevalent in the deeper waters of the reef system along with the massive corals *Porites* spp. on the reef flat.

Heron Reef experiences semidiurnal tides with a spring and neap tidal range of 2.28 and 1.09 m (Chen & Krol, 1997). Wave height on the reef flat is typically <0.5 m under a mean wind speed of 5 m/s, and wave heights are <0.6 times the maximum water level (Gourlay, 1988). When the tide is higher than the reef rim, oceanic waves may travel across the reef flat, resulting in the regional wave climate being the key control of wave action. Occasionally, wind waves are superimposed on low to moderate sea swell produced by the prevailing southeasterly trade winds. Cyclonic storms during late summer that are concurrent with king tides may cause large waves to travel over the reef.

3. Instrumentation

Quantification of energy exchanges over marine environments through direct measurement presents many challenges, particularly the maintenance of equipment and correction of data for wave motion of sensor platforms. Historically, this has resulted in observations over coral reefs being made from shorelines or from masts built into coral reefs (Garratt & Hyson, 1975; Tanaka et al., 2008). Both approaches have their own limitations, such as confining measurement periods to specific wind directions, variable sensor heights above the water surface due to tidal cycles, and damage to fragile corals.

As a consequence, direct measurement of energy and trace gas exchanges over Heron Reef was made by eddy covariance systems deployed on moored pontoons between 2005 and 2010 (Figure 3). Weibe et al. (2011) demonstrated that this approach was robust, with vertical wave motion (p') on Heron Reef not showing strong coherency with vertical wind speed (w') when monitored by a Campbell Scientific CSAT 3 sonic anemometer on a moored pontoon. Interaction found between the two spectra was greater than an order of magnitude below the measured fluctuations, so that over an averaging period of 30 min, small-scale wave-induced motion of the pontoon did not influence measurements of turbulent fluxes (Weibe et al., 2011). The results of Weibe et al. (2011) are supported by those of Eugster et al. (2003), Vesala et al. (2006), Nordbo et al. (2011), and McJannet et al. (2013) who also successfully deployed eddy covariance systems on pontoons on lakes and reservoirs in wave energy environments more similar to those found over a coral reef than the open ocean. Deployment of eddy covariance instrumentation on pontoons is particularly appealing over coral reefs, as it can be deployed and retrieved manually without causing damage to fragile

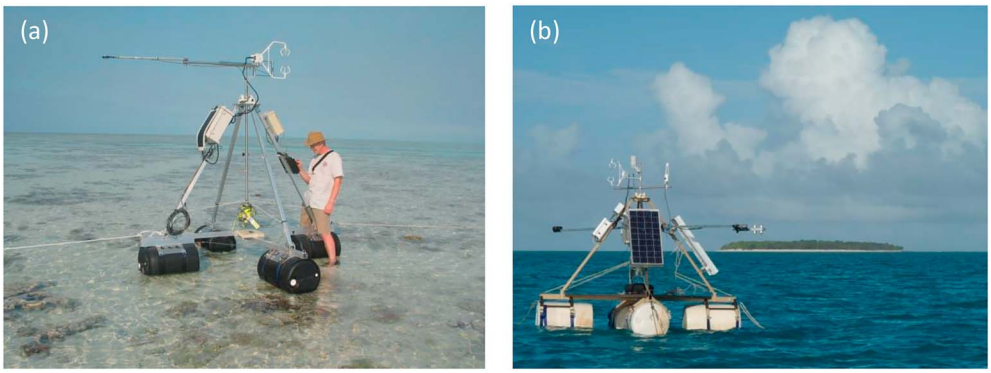

Figure 3. Eddy covariance pontoon moored over (a) the Reef Flat site, Heron Reef, in February 2007 and (b) the deep lagoon in February 2010 (Figure 2).

corals, while in deeper water the pontoons can be maneuvered easily and retrieved quickly before onset of severe weather (see McGowan et al., 2010, 2016; MacKellar & McGowan, 2010; MacKellar, McGowan, & Phinn, 2012).

The first eddy covariance system was deployed on Heron Reef in September 2005 as part of a third year undergraduate student field course in Geography, with a subsequent deployment in February 2007 (Figure 3a). These two measurement periods provided essential proof of concept with convective flux data compared with that collected by an eddy covariance system installed on the windward shoreline of Heron Island, allowing assessment of the possible influence of wave motion on eddy covariance measurements (McGowan et al., 2010; Weibe et al., 2011).

Improvements to the design of the pontoon and mounting of instrumentation were implemented in the manufacture of second-generation pontoons deployed during measurement programs from 2008 to 2010. The pontoon frames onto which the eddy covariance units were mounted consisted of two 2.5-m (3.5-m, second generation) aluminum crossbars with a 120-dm^3 (250-dm^3, second generation) drum attached at each end (Figure 3b). The sensors were attached to a mast suspended above the center of the pontoon by a gimbal mounted on a supporting frame. The gimbal was designed to lessen the influence of wave action on the position of the sensors so that they remained near level at a constant height of ~2.15 m above the water surface. Elastic cords connected the base of the mast to the pontoon frame to further dampen any motion caused by wave action. The pontoon was held in position using four mooring lines attached to the end of each crossbar. This meant that the pontoon was able to rise and fall with the tides while maintaining its general orientation (see MacKellar, McGowan, & Phinn, 2012; McGowan et al., 2010).

In this environment, sea spray and associated deposition of salt on sensors (Table 1) necessitates that eddy covariance systems are regularly serviced. At Heron Reef, eddy covariance systems were checked daily for evidence of salt scale on the surfaces of the Li-Cor 7500 open path gas analyzer and radiometers, with instruments washed with freshwater as required to remove salt. During summer, convective showers often crossed the field area, more frequently during periods of active monsoon and also helped wash salt from instrumentation.

A Vaisala CL31 ceilometer was also deployed on Heron Island to continuously monitor cloud height, while Vaisala RS80 radiosondes were deployed during 2009 and 2010 field periods to obtain aerological soundings over Heron Reef. An Onset Hobo RG 3 data logging rain gauge was installed on Heron Island during field campaigns to continuously monitor precipitation. Routine soundings up to heights of 800 m above sea level were made 3 to 6 times per day with a kite mounted tethersonde similar to that described by McGowan and Sturman (1996), flown from the windward shorelines of Heron Island. A custom-made tethersonde measured air temperature, relative humidity, barometric pressure, wind speed, and direction with data transmitted to a surface receiver and laptop computer at 10-s intervals. The tethersonde was flown when wind speeds ranged from 2.5 m/s to around 20 m/s.

3.1. Eddy Covariance Corrections

Typically, measured fluxes of Q_h, Q_e, and Q_g only account for approximately 70–90% of measured Q^* in micrometeorological studies (see, e.g., Heusinkveld et al., 2004). Over a coral reef, the added complexity

Table 1
Instrumentation Deployed on and Adjacent To, Pontoons Over Heron Reef

Instrument	Parameter	Resolution/Accuracy
Campbell Scientific CSAT3 sonic anemometer	u_x, u_y, u_z, speed of sound (c), sonic temperature, wind direction, sensible heat flux	1 mm/s rms (u_x, u_y); 0.5 mm/s rms (u_z); 15 mm/s (0.025 °C) rms (c); 0.06° rms (wind direction—accuracy ±0.7° at 1 m/s; for horizontal wind)
Li-Cor 7500 open path H_2O and CO_2 analyzer; internal temperature; barometric pressure		±2% of reading (H_2O CO_2); ±0.2 °C; ±1.5% of full scale span
Vaisala HMP45A air temperature and relative humidity sensor	Air temperature, relative humidity, vapor pressure	±2% RH (0 ... .90% RH) @20 °C ±3% RH (90 ... .100% RH) @20 °C ±0.2 °C @20 °C
Kipp & Zonen NRLite (2005, 2007)	Net radiation	Spectral range 0.2 to 100 μm
Kipp & Zonen CRN1 (2007 to 2010)	Incoming/outgoing long and short wave radiation	Pyranometer spectral range 0.305 to 2.8 μm/Pyrgeometer spectral range 5 to 50 μm
Campbell CR23X & CR3000 data loggers		Sampling frequency 10 Hz and block averaging at 15 min
HOBO U20–001-01	Water level and water temperature at seabed	0.21 cm; ±0.44 °C
HOBO PROV2 logger	Water temperature	0.02 °C/±0.21 °C

associated with tidal movement of water (vertically), associated horizontal currents (advection), and the morphological complexity of corals and other benthic cover mean that closure of the energy balance by direct measurements of energy fluxes is at present unrealistic. The problem may be further complicated by measurement uncertainty related to instrumentation. For example, daily averages of total net radiation measured by the Kipp and Zonen CNR1 net radiometers deployed on the pontoons (2009 and 2010) were found to have a bias of ~10 W/m^2 for daily average values, which far exceeded the reported accuracies by the manufacturer (Michel et al., 2008). Despite the improbability of attaining energy budget closure, "the strengths of the EC system far outweigh its weaknesses" and it remains the most benchmarked method of determining surface-atmosphere energy exchanges (Baldocchi et al., 2001, p 2418).

Prior to interpretation, all eddy covariance data underwent postprocessing to correct for errors and to remove spurious data. Eddy covariance errors can arise due to tilted instruments, cross contamination of the vertical flux by the other wind components, and/or by instrument-induced turbulent wakes if instrumentation is not accurately aligned with the mean wind direction. A two-dimensional coordinate rotation correction was applied so that the instrument's reference frame was aligned with the streamline coordinates (Lee et al., 2004). This ensures that all derived fluxes are not affected by instrument tilts or flow distortion (Burba & Anderson, 2009).

Corrections were also applied to account for underestimation of fluxes due to the attenuation of eddies of various frequencies (Massman & Lee, 2002). Typically, loss of the true turbulent signal arises due to the separation of sensors, slow sensor response times, sensor design and electronic filters, as well as short averaging periods and signal processing. These errors can account for as much as 5–30% of the measured fluxes and, as such, frequency response corrections were applied to all measured fluxes (Burba & Anderson, 2009).

As detailed in McGowan et al. (2010, 2016) and MacKellar, McGowan, and Phinn (2012) the Webb-Pearman-Leuning (WPL) correction was applied to correct for density effects (Webb et al., 1980) on water vapor and CO_2 measurements. The influence of solar heating of the LI-7500 open path gas analyzers on air density within the instrument's measurement path (Järvi et al., 2009) was corrected for using the decision tree approach of Burba et al. (2008). Specific corrections were applied to day and night CO_2 flux measurements made from 0600 Australian Eastern Standard Time (AEST) to 1815 AEST corresponding to 22 and 24 min after sunrise and sunset, respectively.

Further data quality control involved removal of data spikes identified as statistical outliers caused by electrical noise, nonstationarity or coeval rainfall. Data points were removed when the automatic gain control value of LI-7500 was ≥70% (Liu et al., 2009) to minimize the potential effect of salt spray and rainwater adhering to the lens of the LI-7500 open path gas analyzers (OP-IRGA). Finally, a moving average-based 3σ filter similar to Schmid et al. (2000) was applied across three iterations of processed data to remove remaining data spikes (see McGowan et al., 2016).

3.2. Foot Printing

Eddy covariance measurements are highly susceptible to the influence of nontarget area upwind surfaces. Nonsource area contamination, often due to horizontal advection, can compromise eddy covariance data quality and the usefulness of sampling heterogeneous environments such as over the surface of coral reefs. Thus, accurate foot printing is essential in order to identify the area of influence on flux measurements—specifically whether the influence of the surrounding ocean or adjacent reef zone, that is, reef flat, shallow lagoon, deep lagoon, has extended onto the source flux surface of interest.

On Heron Reef, measurement foot printing was achieved using a model developed by Isaac (2004), which employs the Horst and Weil (1992) model for the crosswind component and functions for predicting the upwind dimension by Schmid (1994). This widely used approach was chosen because it includes an atmospheric stability correction function (ψm) and provides a reliable 3-D representation of the flux source area as detailed in McGowan et al. (2016), and references therein.

4. Insights Into Surface—Atmosphere Energetics at Heron Reef

4.1. Surface Energy Balance

Our initial measurements of the surface energy balance were made in September 2005 (spring), later in February 2007 (summer) and in July 2007 (winter) over the reef flat about 150 m east of Heron Island (Figure 2). In stark contrast to energy balance partitioning described in the literature for the open ocean, where up to 90% of net radiation (Q^*) is partitioned into Q_e resulting in annual Bowen ratio (Q_h/Q_e) values of ~0.10 (Oke, 1978), over the reef flat at Heron Reef up to 80% of Q^* was partitioned into storage (ΔQ_{swr}; McGowan et al., 2010). These results are similar to Tanaka et al. (2008), who found ~70% of Q^* went into storage during late summer, either heating the water overlying the reef flat and/or the reef substrate at the subtropical location of Miyako Island, Japan (24.91°N; 125.26°E). Collectively, these observations highlight the importance of radiation exchanges in the energetics of the shallow water environments of coral reefs and that the thermal properties of shallow reef waters may be more influenced by local radiation exchanges and meteorology than larger scale surrounding oceanic water temperatures. Understanding the controls of the thermal environment of coral reefs and establishing the correct relative attributions to water temperature overlying coral reefs is essential to inform debate on causes of coral bleaching, and the interpretations of palaeo-reef temperatures reconstructed from ancient corals.

From 18 to 22 February 2009 eddy covariance observations were made over Heron Reef during conditions that resulted in coral bleaching. This period was characterized by predominantly cloudless skies, light northeast winds averaging 2.6 m/s with air temperatures from 24.8 to 29.2 °C. Water surface and bottom temperatures in days prior to 18 February 2009 were between 26 and 28 °C (MacKellar & McGowan, 2010). During the measurement period net radiation peaked at between 786 to 887 W/m^2 at around 1200 AEST daily, with up to 93% to 95% of Q^* partitioned into ΔQ_{swr} during the mornings coinciding with low tide. As a result, water temperatures over the reef increased quickly, reaching >34 °C between 1500 and 1700 AEST, well in excess of the upper thermal tolerance of most corals of ~30 °C (Hoegh-Guldberg, 1999), as detailed in MacKellar and McGowan (2010). Latent heat flux and Q_h peaked daily in the late afternoon and evening corresponding with peaks in wind speed of around 5 m/s, surface friction velocity and maximum air-sea temperature difference (>5 °C at around 1600 AEST).

Measurements of radiation exchanges during this period highlighted net solar radiation as the major cause of radiative heating of water overlying the reef, with mean daily net shortwave radiation (K^*) of 70.55 MJ·m^{-2}·day^{-1} and mean daily net longwave radiation (L^*) of −17.73 MJ·m^{-2}·day^{-1}. This was combined with light winds and high absolute humidity, ranging from 20 to 23 g/m^3, which limited the potential for evaporative cooling of reef waters and low midday tides, so that water overlying the reef warmed quickly from around 28 °C at 0900 AEST to ~35 °C by late afternoon. This period of extreme heating of waters overlying the reef highlights the importance of low tides around solar noon combining with light winds, high absolute humidity, and clear skies in causing rapid heating of reefs. These results are consistent with Smith (2001) who also found that bleaching events were common during periods of low wind speeds, low Q_e and Q_h and therefore little evaporative cooling of reef surface waters. Collectively, these conditions result in the buildup of heat in the shallow waters overlying coral reefs with water temperatures far exceeding those of the surrounding

Table 2
Mean Radiation and Turbulent Fluxes for Three Observation Periods at Heron Reef, February 2010

	OP1 (0000 UTC 4 Feb to 0500 UTC 7 Feb 2010)		OP2 (0530 UTC 7 Feb to 0700 UTC 12 Feb 2010		OP3 (0730 UTC 12 Feb to 1230 UTC 13 Feb 2010	
Mean flux (W/m)	Reef flat	Shallow lagoon	Reef flat	Deep lagoon	Reef flat	Ocean site
$L\uparrow$	458	458	460	459	461	461
$L\downarrow$	413	414	411	410	396	394
$K\uparrow$	32	30	42	28	42	20
$K\downarrow$	242	249	268	267	369	390
α	0.13	0.12	0.16	0.10	0.11	0.05
Q^*	165	175	177	189	261	303
Q_E	85	102	138	192	116	118
Q_H	7	5	16	15	8	4
Q_{SWR}	74	67	23	−18	137	181
β	0.08	0.05	0.16	0.08	0.07	0.03
D	0.9	2.7	0.8	3.1	1	11

Note. Also listed is the Bowen Ratio (β), albedo (α), and water depth in meters (D) (Modified after MacKellar, McGowan, & Phinn, 2012).

ocean. Results also highlight the relative role of reef scale (meters to kilometers) energy balances compared to global scale gradual warming of oceans in causing extreme water temperatures on coral reefs.

The morphological and hydrodynamic complexity of coral reefs means that their surface energy balance should display similarly heterogeneous characteristics. However, studies of simultaneous energy transfers over different reef environments are rare, leading to point measurements from one site often being considered representative of an entire coral reef. In February 2010 two eddy covariance systems were operated concurrently from 3 to 13 February at Heron Reef with one system providing continuous measurements over the reef flat and the other system operated over the shallow lagoon, deep lagoon, and open ocean. Although observations were only able to provide comparisons between sites for a few days each, they highlighted the heterogeneity of the surface energy balance across the coral reef.

Shallow water environments over the reef flat were found to act as a net sink of energy while deeper water sites on the reef were a net source of energy to the atmosphere (MacKellar, McGowan, & Phinn, 2012), primarily through evaporation associated with increased wind speed and wave height. Mean daytime albedos over the reef flat, where coral sand and rubble comprised around 70% of the benthic assemblage, were 10%, 26%, and 45% higher than the shallow lagoon, deep lagoon, and adjacent ocean, respectively. The higher reflectance of shortwave radiation over the reef flat resulted in lower overall available Q^*, which was found to range from 165 to 261 W/m^2. This is similar to summertime Q^* reported for coral reefs by Kjerfve (1978) in the Caribbean and Tanaka et al. (2008) at Miyako Island, Japan. In the deeper waters of the shallow and deep lagoons Q_e was strongly correlated ($R^2 = 0.25$ to 0.69, respectively) with wind speed. Table 2 presents the mean radiation and energy fluxes recorded during this period of concurrent observations at different sites across Heron Reef. Also listed are the mean water depths, albedos and Bowen ratios, with the deep lagoon being the only site during the study period to be a net source of energy to the overlying air (during OP2; Table 2). The higher albedos monitored over the Reef Flat and Shallow Lagoon sites highlight the role of the white coral sand in reflecting solar radiation back through the overlying water at mean depths up to at least 2.7 m. Bowen ratios were similar across all sites except at the Reef Flat during OP2 when it was monitored to be 2 times greater than during OP1 and OP3. This reflects the higher mean Q_h value during this period due to lower daytime water levels which resulted in higher water temperatures (MacKellar, McGowan, & Phinn, 2012).

The drag coefficient C_D, which represents the total air-sea momentum flux (Hasse & Smith, 1997), calculated for the measurement height of 2.2 m and corrected for stability following Hsu (1988) for sites over Heron Reef ranged from 1.5×10^{-3} to 2.3×10^{-3}. Its relationship with wind speed averaged across the Reef Flat, Shallow and Deep Lagoon sites from approximately 600 hr of data was found to be best represented by the linear function $C_D = 0.001u + 0.0013$ where u is mean 30-min wind speed at 2.2 m above the water

surface, which gave an R^2 value of 0.99. The C_D values calculated for Heron Reef are similar to the rare reports of C_D over coral reefs in the literature by Tsukamoto et al. (1991), and from Garratt and Hyson (1975) almost 50 years ago. The drag coefficient over reef flats may be influenced by the emergence of roughness elements at low tide as corals extend above the water surface, and in response to changing wind speeds and wave conditions. Given the importance of understanding momentum and its accurate parameterization in modeling air-sea energy exchanges, it is crucial that additional studies are made of C_D under the widest possible range of conditions.

4.2. CO_2 Flux

Air-sea CO_2 exchange as described in McGowan et al. (2016) was monitored throughout the deployment of eddy covariance systems on Heron Reef. This provided representative measurements of CO_2 transfers for the first time at the scale of biogeomorphic systems (i.e., hectares) under a wide range of meteorological and hydrodynamic conditions. Eddy covariance is one of the most accurate ways to determine CO_2 flux, albeit not without difficulty in harsh marine settings (Wanninkhof et al., 2009). Previously, CO_2 exchanges with the atmosphere over coral reefs have been quantified using chamber-based measurements covering less than 1 m^2. Others have centered on quantifying the CO_2 partial pressure (pCO_2) gradient between the water surface and the lower atmosphere and then calculating the gas transfer velocity as a function of wind speed (i.e., Kayanne et al., 1995; Kondo & Tsukamoto, 2012; Massaro et al., 2012; Yan et al., 2011); or through biological productivity modeling (Gattuso et al., 1996, 1999). Results from these studies have then often been inferred to be representative of much larger areas or the whole of reef systems, thereby neglecting the heterogeneous properties of coral reefs. Our case study observations made from 3 to 13 February 2010 found that the reef flat was a net source of CO_2 to the atmosphere with a mean efflux of 0.088 $mg{\cdot}m^{-2}{\cdot}s^{-1}$. Concurrent measurements over the shallow and deep lagoon areas confirmed these regions to be net sinks of CO_2 with mean values of 0.1 $mg{\cdot}m^{-2}{\cdot}s^{-1}$ and 0.27 $mg{\cdot}m^{-2}{\cdot}s^{-1}$, respectively (see McGowan et al., 2016). As with our observations of the surface energy balance, CO_2 exchanges over Heron Reef displayed distinct zonation reflecting the underlying geomorphic and ecological characteristics of the coral reef.

Understanding CO_2 exchanges with the atmosphere over coral reefs is crucial to establishing their role in global carbon budgets, biogeochemical cycles, climate change, and the impact of rising atmospheric CO_2 concentrations on ocean acidification. Previous studies have concluded that coral reefs are net sinks of CO_2 (Kayanne et al., 1995), while others have found them to be net sources (Kawahata et al., 1997, 1999; Yan et al., 2011). Our research indicates that CO_2 exchanges with the atmosphere over coral reefs are influenced by a multitude of factors. These include water depth, wave action, the benthic assemblage of corals and rubble, tidal currents, and proximity to shorelines where hydraulic pumping of sands by tidal fluctuations may lead also to drainage of freshwater from islands onto reefs, all influencing CO_2 fluxes (McGowan et al., 2016). Accordingly, a whole of system and multidisciplinary approach to quantification of air-sea CO_2 exchanges over coral reefs is needed to establish their role as a blue carbon ecosystem.

4.3. Insights Into Coral Bleaching

While many environmental stressors such as pollution, sedimentation from coastal run-off, over fishing, and invasion of pests onto coral reefs may trigger bleaching, the most extensive and damaging bleaching occurs when water temperatures exceed the thermal tolerance of corals. These conditions have been linked to global warming and ENSO events, with global bleaching events becoming more frequent in the past 20 years, including the back-to-back global bleaching events of 2016 and 2017 (Baker et al., 2008; Hughes et al., 2017; Kleypas et al., 2015). However, reef scale energetics during a coral bleaching event including radiation transfers and exchanges of Q_e and Q_h had never been investigated prior to our research on Heron Reef (MacKellar & McGowan, 2010). Instead, the correlation between rising global atmospheric and oceanic water temperatures and more frequent coral bleaching events was widely considered to be evidence enough of causation (Hoegh-Guldberg, 1999; Hoegh-Guldberg et al., 2007).

During the field measurement campaign from 18 to 22 February 2009 (MacKellar & McGowan, 2010), water temperatures on Heron Reef were observed to exceed 34 °C, well above the widely acknowledged thermal tolerance of most coral species of around 30 °C (Hoegh-Guldberg et al., 2007). The meteorology at the time was characterized by light winds, high humidity, and clear skies with low tides occurring at midday. Daily Q^*

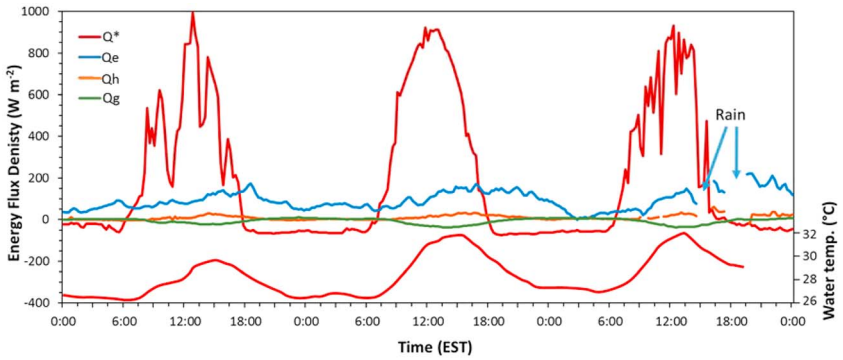

Figure 4. Eddy covariance measurements made from 5 to 7 February 2010 over a reef flat site similar to that shown in Figure 3a.

peaked at around 800 W/m^2 with >93% partitioned into heating the water, benthos, and substrate. Latent heat fluxes peaked in the early evening following sunset at around 200 W/m^2 with maximum wind speeds contributing to a loss of energy from the water overlying the reef with a corresponding decrease in water temperature due to evaporative cooling. These first direct measurements of radiation exchanges and energy flux partitioning over a coral reef during a coral bleaching event highlighted the importance of prevailing synoptic conditions of weak pressure gradients (lights winds), clear skies, high air temperatures, and humidity providing favorable conditions for the buildup of heat in water overlying the reef, similar to the findings by Smith (2001) and Mumby et al. (2001).

From 3 to 13 February 2010 a second period of extreme heating of water overlying the reef was observed by eddy covariance systems deployed at Heron Reef. Figure 4 presents measurements made from 5 to 7 February 2010 when maximum water temperatures reached 32 °C. Daily Q^* peaked between 900 and 1,000 W/m^2 as a result of scattered cloud enhancing solar radiation receipt at the reef surface through downward reflection of direct beam radiation by the sides of the clouds. During this period heat flux plates were also installed into coral sand on the reef floor in a first attempt to quantify the heat flux between the water overlying the reef and the underlying reef substrate (Figure 4).

In Figure 4 the impact of cloud on measured Q^*, Q_h, and Q_e can be clearly seen on 5 and 7 February when the field site was also affected by showers. Over the 3-day period Q_e peaked each day at around 1800 EST between 170 and 200 W/m^2, coinciding with maximum wind speeds (not shown). Sensible heat flux peaked at around 3 hr following solar noon (1500 EST) at approximately 30 W/m^2 with heat flux into the coral sand (Q_g) measured at −4 cm below the sand surface, being slightly greater at around 35 W/m^2. While caution is needed in interpreting the significance of these first Q_g measurements, they do suggest that heat transfer into coral sand may at least be equivalent to Q_h with the atmosphere in shallow water reef flat settings. Further research is needed to validate these initial results and to develop methods to extend such measurements to more complex benthic environments on reefs. Water temperatures during this period are shown to have trended upward over the 3 days reaching a maximum on 7 February (Figure 4) before increased shower activity and strong winds over the following days lowered water temperatures. Nonetheless, isolated coral bleaching was observed on the reef flat at Heron Reef following this 3-day period.

Using the understanding of the meteorology associated with observed coral bleaching events at Heron Reef, a synoptic climatology of coral bleaching events on the GBR was developed following the methods of Yarnal (1993) and Theobald et al. (2015). Here an automated *k*-means clustering method for weather typing using multiple variables [sea level pressure (MSLP), surface (2 m) air temperature (SAT), surface (10 m) wind vectors, total cloud cover (TCC; surface), and high cloud cover (HCC; > ~500 hPa)] was applied using ERA-Interim reanalysis data at 0.4° resolution for the GBR including Heron Island.

Results of the study identified seven synoptic weather types that dominate during coral bleaching events. The most common type is associated with above average mean sea level pressure, higher surface air temperatures, negative cloud cover anomalies, and high humidity. Under these conditions water temperatures over

Figure 5. Commencing an aerological sounding using a kite flown tethersonde on the eastern shoreline of Heron Island.

individual coral reefs are typically >2 °C above average (McGowan & Theobald, 2017), similar to conditions found during energy balance observations at Heron Island in February 2010 when coral bleaching occurred. Accordingly, these studies highlight the role of atmospheric processes at the synoptic scale in controlling the energy balance of individual coral reefs at micro to local scales over hours and hundreds of meters, rather than ENSO or background warming of the oceans.

4.4. Convective Coral Reef Internal Boundary Layer

Tethersonde flights conducted over Heron Reef (Figure 5) identified the development of convective internal boundary layers (CIBL) during both winter and summer conditions (MacKellar, McGowan, Phinn, & Soderholm, 2012). The reef CIBL develops as oceanic marine air moves across the ocean-reef boundary growing via entrainment of heat and moisture from the underlying warmer waters overlying the coral reef. The CIBL was observed to reach a maximum height of around 130 m at 5 to 8 km downwind of the ocean-reef boundary. An example of a typical wintertime CIBL measured over Heron Reef by a kite-based tethersonde sounding at 11:50 AEST on 11 June 2009 is presented in Figure 6. The unstable surface CIBL reef air is 65-m deep and is clearly distinguishable in the virtual potential temperature and mixing ratio profiles. Above this layer the regional marine boundary layer displays a drier neutral profile with wind speeds around 6 to 8 m/s. Surface energy balance observations over the reef flat at this time measured by the eddy covariance system were Q_e 230 W/m^2 and Q_h 74 W/m^2, with Q^* at 520 W/m^2, indicating transfer of heat from the reef to the overlying air, primarily via evaporation. Evaporation over warm coral reef waters in convectively unstable atmospheres, particularly during summer, is well known to lead to cumulus clouds over coral reefs, including over Heron Reef. These clouds and at times precipitation cause negative feedback, reducing incoming solar radiation and cooling surface waters including through the addition of fresh rainwater. Accordingly, the reduction in the temperature of water overlying the reef increases the stability of the surface air layer which has been observed to coincide with clearing skies.

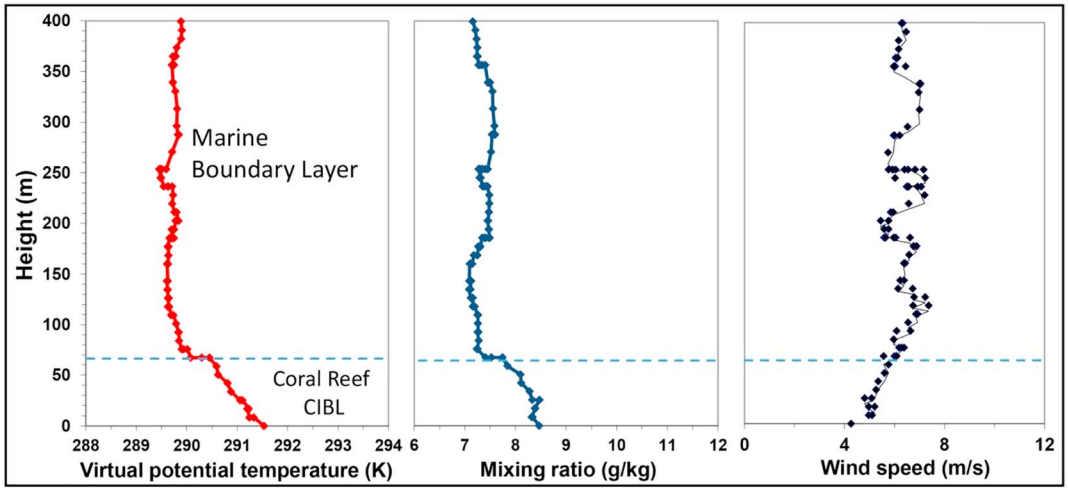

Figure 6. Vertical profiles of virtual potential temperature (θv), mixing ratio, and wind speed measured over Heron Reef at 11:50 AEST, 11 June 2009.

5. Future Directions

Coral reefs face an uncertain future due to coastal development, illegal and destructive fishing practices, contaminated run-off from agriculture and urban areas, invasion by exotic pests, ocean acidification, and global warming. However, the meteorology of these rainforests of the tropical and subtropical oceans remains largely unknown. Here we have summarized observations from a decade of research conducted at Heron Reef in the southern Great Barrier Reef, Australia. Results highlight the distinctly different characteristics of the energy balance of these shallow water marine environments compared to the surrounding ocean. In particular, we have shown that the majority of Q^* is partitioned into heating of waters overlying coral reefs, the benthos and reef substrate. In comparison, over the open oceans more than 50–90% of Q^* is partitioned into Q_e. This characteristic of coral reefs means that not only are they naturally warmer than the surrounding ocean but that changes in synoptic meteorology that influence cloud cover and therefore incoming solar radiation, wind speed, and humidity may have rapid and arguably disproportionate effects on the thermal environment of coral reefs. Further research in this area is strongly recommended to address the dearth of concurrent energy balance measurements over coral reefs and adjacent oceans. Accordingly, research on coral bleaching should consider changes in regional and synoptic scale atmospheric circulation, whether in response to larger-scale forcing such as ENSO or global warming. Results of these efforts may improve prediction of areas likely to experience extreme warming of water overlying coral reefs and help focus management actions on those more vulnerable areas.

With regard to the measurement of energy exchanges over coral reefs, quantification of ΔQ_a and Q_g should be a priority. We suggest that such work includes both field and laboratory studies, initially to explore methods to quantify heat transfer in branching and massive corals, while high-frequency three-dimensional current meters and temperature sensors should be deployed with pontoon-mounted eddy covariance systems to quantify ΔQ_a. At Heron Reef we deployed heat flux plates in the sands of the lagoon, a method that while showing promise to quantify a component of Q_g requires further testing.

Our pilot study observations of CO_2 exchange with the atmosphere using eddy covariance measurements over Heron Reef highlighted the spatial heterogeneity of CO_2 fluxes, reflecting different biophysical conditions on the reef. As a result, future studies of the role of coral reefs in CO_2 budgets should use eddy covariance to enable representative direct measurement of CO_2 exchanges with the atmosphere over large areas. With careful planning and consideration of measurement footprints these studies can be tailored to specific zones on a reef where reef ecology, hydrology, and geomorphology are known.

Finally, Heron Reef is located in the subtropics on the southern margins of the GBR, while other rare studies have been conducted in the Caribbean, South China Sea, Hawaii, and Red Sea. Accordingly, there is a clear need to extend research of the micrometeorology of coral reefs to other locations such as the tropical Pacific and Indian Oceans, where different background meteorology including monsoons and surrounding oceanic conditions occur. Using observations of the interactions between coral reefs and the atmosphere should then underpin high-resolution numerical modeling of the influence of coral reefs on coastal meteorology including effects on winds, cloud, and precipitation. The potential influence on tropical storms would seem worthy of significant focus given potential for feedback processes whereby warm reef waters may contribute to storm development and intensity, which in turn moderates reef temperatures as a result of cloud cover, rainfall, and mixing of cooler ocean waters into the lagoons of coral reefs.

Acknowledgments
Research was conducted at Heron Reef on the southern Greater Barrier Reef under Permit G09/3033.1. The authors are most grateful for financial and technical support received from their host institutions and for assistance in the field and with data analysis provided by Michael Gray, Stuart Phinn, Joshua Soderholm, Glenn Ewels, and David Neil. Access to data referred to in this article can be arranged by contacting the corresponding author or via this site (https://doi.org/10.14264/uql.2019.14).

References

Baker, A. C., Glynn, P. W., & Riegl, B. (2008). Climate change and coral reef bleaching: An ecological assessment of long-term impacts, recovery trends and future outlook. *Estuarine, Coastal and Shelf Science*, *80*(4), 435–471. https://doi.org/10.1016/j.ecss.2008.09.003

Baldocchi, D., Falge, E., Gu, L., Olson, R., Hollinger, D., Running, S., et al. (2001). FLUXNET: A new tool to study the temporal and spatial variability of ecosystem-scale carbon dioxide, water vapor, and energy flux densities. *Bulletin of the American Meteorological Society*, *82*(11), 2415–2434. https://doi.org/10.1175/1520-0477(2001)082<2415:FANTTS>2.3.CO;2

Beringer, J., Hutley, L. B., McHugh, I., Arndt, S. K., Campbell, D., Cleugh, H. A., et al. (2016). An introduction to the Australian and New Zealand flux tower network—OzFlux. *Biogeosciences*, *13*(21), 5895–5916. https://doi.org/10.5194/bg-13-5895-2016

Brown, B. E. (1997). Coral bleaching: Causes and consequences. *Coral Reefs*, *16*, 129–138.

Burba, G., & Anderson, D. (2009). *A brief practical guide to eddy covariance flux measurements: Principles and workflow examples for scientific and industrial applications*. Lincoln, USA: LI-COR Biosciences. https://doi.org/10.13140/RG.2.1.1626.4161

Burba, G. G., McDermitt, D. K., Grelle, A., Anderson, D. J., & Xu, L. (2008). Addressing the influence of instrument surface heat exchange on the measurements of CO_2 flux from open-path gas analyzers. *Global Change Biology*, *14*(8), 1854–1876. https://doi.org/10.1111/j.1365-2486.2008.01606.x

Butterworth, B. J., & Miller, S. D. (2016). Automated underway eddy covariance system for air-sea momentum, heat, and CO_2 fluxes in the Southern Ocean. *Journal of Atmospheric and Oceanic Technology*, *33*(4), 635–652. https://doi.org/10.1175/JTECH-D-15-0156.1

Chen, D., & Krol, A. (1997). Hydrogeology of Heron Island, Great Barrier Reef, Australia. In H. L. Vacher, & T. Quinn (Eds.), *Geology and Hydrogeology of Carbonate Islands. Developments in Sedimentology* (Vol. 54, pp. 867–884). New York: Elsevier Sci.

Claar, D. C., Szostek, L., McDevitt-Irwin, J. M., Schanze, J. J., & Baum, J. K. (2018). Global patterns and impacts of El Niño events on coral reefs: A meta-analysis. *PLoS ONE*, *13*(2), e0190957. https://doi.org/10.1371/journal.pone.0190957

Davis, K., Lentz, S., Pineda, J., Farrar, J., Starczak, V., & Churchill, J. (2011). Observations of the thermal environment on Red Sea platform reefs: A heat budget analysis. *Coral Reefs*, *30*(S1), 25–36. https://doi.org/10.1007/s00338-011-0740-8

Eugster, W., Kling, G., Jonas, T., McFadden, J. P., Wüest, A., MacIntyre, S., & Chapin, F. S. III (2003). CO_2 exchange between air and water in an Arctic Alaskan and mid-latitude Swiss lake: Importance of convective mixing. *Journal of Geophysical Research*, *108*(D12), 4362. https://doi.org/10.1029/2002JD002653

Frieler, K., Meinshausen, M., Golly, A., Mengel, M., Lebek, K., Donner, S. D., & Hoegh-Guldberg, O. (2013). Limiting global warming to 2 °C is unlikely to save most coral reefs. *Nature Climate Change*, *3*(2), 165–170. https://doi.org/10.1038/nclimate1674

Garratt, J. R., & Hyson, P. (1975). Vertical fluxes of momentum and sensible heat and water vapour during the Air Mass Transformation Experiment (AMTEX) 1974. *Journal of the Meteorological Society of Japan*, *53*(2), 149–160. https://doi.org/10.2151/jmsj1965.53.2_149

Gattuso, J.-P., Frankignoulle, M., & Smith, S. V. (1999). Measurement of community metabolism and significance in the coral reef CO_2 source-sink debate. *Proceedings of the National Academy of Sciences of the United States of America*, *96*(23), 13,017–13,022. https://doi.org/10.1073/pnas.96.23.13017

Gattuso, J.-P., Pichon, M. R., Delesalle, B., Canon, C., Copin-Montegut, G., Pichon, M., & Frankignoulle, M. (1996). Carbon fluxes in coral reefs. I. Lagrangian measurements of community metabolism and resulting air-sea CO_2 disequilibrium. *Marine Ecology Progress Series*, *145*, 109–121. https://doi.org/10.3354/meps145109

Gourlay, M. R. (1988). Coral Cays' products of wave action and geological processes in a biogenic environment. In *Proc. 6th Int. Coral Reef Symposium* (pp. 491–496). Townsville, Australia: Great Barrier Reef Committee.

Hasse, L., & Smith, S. D. (1997). Local sea surface wind, wind stress, and sensible and latent heat fluxes. *Journal of Climate*, *10*(11), 2711–2724. https://doi.org/10.1175/1520-0442(1997)010<2711:LSSWWS>2.0.CO;2

Heusinkveld, B. G., Jacobs, A. F. G., Holtslag, A. A. M., & Berkowicz, S. M. (2004). Surface energy balance closure in an arid region: Role of soil and heat flux. *Agricultural and Forest Meteorology*, *122*(1-2), 21–37. https://doi.org/10.1016/j.agrformet.2003.09.005

Hoegh-Guldberg, O. (1999). Climate change, coral bleaching and the future of the world's coral reefs. *Marine and Freshwater Research*, *50*(8), 839–866. https://doi.org/10.1071/MF99078

Hoegh-Guldberg, O., Mumby, P. J., Hooten, A. J., Steneck, R. S., Greenfield, P., Gomez, E., et al. (2007). Coral reefs under rapid climate change and ocean acidification. *Science*, *318*(5857), 1737–1742. https://doi.org/10.1126/science.1152509

Hollinger, D. Y., Goltz, S. M., Davidson, E. A., Lee, J. T., Tu, K., & Valentine, H. T. (1999). Seasonal patterns and environmental control of carbon dioxide and water vapour exchange in an ecotonal boreal forest. *Global Change Biology*, *5*(8), 891–902. https://doi.org/10.1046/j.1365-2486.1999.00281.x

Hopley, D., Smither, S. G., & Parnell, K. E. (2007). *Geomorphology of the Great Barrier Reef* (Vol. 532). Cambridge: Cambridge University Press. https://doi.org/10.1017/CBO9780511535543

Horst, T. W., & Weil, J. C. (1992). Footprint estimation for scalar flux measurements in the atmospheric surface layer. *Boundary-Layer Meteorology*, *59*(3), 279–296. https://doi.org/10.1007/BF00119817

Hsu, S. A. (1988). *Coastal meteorology* (p. 260). London: Academic Press.

Hughes, T. P., Kerry, J. T., Álvarez-Noriega, M., Álvarez-Romero, J. G., Anderson, K. D., Baird, A. H., et al. (2017). Global warming and recurrent mass bleaching of corals. *Nature*, *543*(7645), 373–377. https://doi.org/10.1038/nature21707

Isaac, P. R. (2004). Estimating surface-atmosphere exchange at regional scales, PhD thesis, 310 pp., School of Chem., Phys. and Earth Sci., Fac.of Sci. and Eng., The Flinders Univ. of Southern Australia. [Available at http://theses.flinders.edu.au/public/adt-FU20060412.170700/.]

Järvi, L., Mammarella, L., Eugster, W., Ibrom, A., Siivola, E., Dellwik, E., et al. (2009). Comparison of net CO_2 fluxes measured with open- and closed-path infrared gas analyzers in urban complex environment. *Boreal Environment Research*, *14*, 499–514.

Jell, J. S., & Flood, P. G. (1978). Guide to the geology of reefs of the Capricorn and Bunker Groups, Great Barrier Reef province (with special reference to Heron Reef). *Papers, Dept. Geol. Univ. Queensland*, *8*(3), 1–85.

Kawahata, H., Suzuki, A., & Goto, K. (1997). Coral reef ecosystems as a source of atmospheric CO_2: Evidence from pCO_2 measurements of surface waters. *Coral Reefs*, *16*(4), 261–266. https://doi.org/10.1007/s003380050082

Kawahata, H., Suzuki, A., & Goto, K. (1999). Coral reefs as source of atmospheric CO_2—Spatial distribution of pCO_2 in Majuro atoll. *Geochemical Journal*, *33*(5), 295–303. https://doi.org/10.2343/geochemj.33.295

Kayanne, H., Suzuki, A., & Saito, H. (1995). Diurnal changes in the partial pressure of carbon dioxide in coral reef water. *Science*, *269*(5221), 214–216. https://doi.org/10.1126/science.269.5221.214

Kjerfve, B. (1978). Diurnal energy-balance of a Caribbean barrier reef environment. *Bulletin of Marine Science*, *28*, 137–145.

Kleypas, J. A., Castruccio, F. S., Curchitser, E. N., & McLeod, E. (2015). The impact of ENSO on coral heat stress in the western equatorial Pacific. *Global Change Biology*, *21*(7), 2525–2539. https://doi.org/10.1111/gcb.12881

Kondo, F., & Tsukamoto, O. (2012). Comparative CO_2 flux measurements by eddy covariance technique using open- and closed-path gas analysers over the equatorial Pacific Ocean. *Tellus, Series B*, *64*(1), 511. https://doi.org/10.3402/tellusb.v64i0.17511

Lee, X., Finnigan, J., & Paw, U. (2004). Coordinate systems and flux bias error. In X. Lee, W. Massman, & B. Law (Eds.), *Handbook of micrometeorology, a guide for surface flux measurement and analysis* (pp. 33–66). New York: Kluwer Academic Publisher.

Liu, H. P., Zhang, Y., Liu, S. H., Jiang, H. M., Sheng, L., & Williams, Q. L. (2009). Eddy covariance measurements of surface energy budget and evaporation in a cool season over southern open water in Mississippi. *Journal of Geophysical Research*, *114*, D04110. https://doi.org/10.1029/2008JD010891

MacKellar, M. C., & McGowan, H. A. (2010). Air-sea energy exchanges measured by eddy covariance during a localised coral bleaching event, Heron Reef, Great Barrier Reef, Australia. *Geophysical Research Letters*, *37*, L24703. https://doi.org/10.1029/2010GL045291

MacKellar, M. C., McGowan, H. A., & Phinn, S. R. (2012). Spatial heterogeneity of air-sea energy fluxes over a coral reef, Heron Reef, Australia. *Journal of Applied Meteorology and Climatology*, *51*(7), 1353–1370. https://doi.org/10.1175/JAMC-D-11-0120.1

MacKellar, M. C., McGowan, H. A., Phinn, S. R., & Soderholm, J. S. (2012). Observations of surface energy fluxes and boundary-layer structure over Heron Reef, Great Barrier Reef, Australia. *Boundary-Layer Meteorology*, *146*(2), 319–340.

Massaro, R. F. S., De Carlo, E. H., Drupp, P. S., Mackenzie, F. T., Jones, S. M., Shamberger, K. E., et al. (2012). Multiple factors driving variability of CO_2 exchange between the ocean and atmosphere in a tropical coral reef environment. *Aquatic Geochemistry*, *18*(4), 357–386. https://doi.org/10.1007/s10498-012-9170-7

Massman, W. J., & Lee, X. (2002). Eddy covariance flux corrections and uncertainties in long-term studies of carbon and energy exchanges. *Agricultural and Forest Meteorology*, *113*(1-4), 121–144. https://doi.org/10.1016/S0168-1923(02)00105-3

McCabe, R., Estrade, P., Middleton, J., Melville, W., Roughan, M., & Lenain, L. (2010). Temperature variability in a shallow, tidally-isolated coral reef lagoon. *Journal of Geophysical Research*, *115*, C12011. https://doi.org/10.1029/2009JC006023

McGillis, W. R., Edson, J. B., Zappa, C. J., Ware, J. D., McKenna, S. P., Terray, E. A., et al. (2004). Air-sea CO_2 exchange in the equatorial Pacific. *Journal of Geophysical Research*, *109*, C08S02. https://doi.org/10.1029/2003JC002256

McGowan, H., & Theobald, A. (2017). ENSO weather and coral bleaching on the Great Barrier Reef, Australia. *Geophysical Research Letters*, *44*, 10,601–10,607. https://doi.org/10.1002/2017GL074877

McGowan, H. A., MacKellar, M. C., & Gray, M. A. (2016). Direct measurements of air-sea CO_2 exchange over a coral reef. *Geophysical Research Letters*, *43*, 4602–4608. https://doi.org/10.1002/2016GL068772

McGowan, H. A., & Sturman, A. P. (1996). A kite based atmospheric sounding system. *Boundary-Layer Meteorology*, *77*, 395–399.

McGowan, H. A., Sturman, A. P., MacKellar, M. C., Wiebe, A. H., & Neil, D. T. (2010). Measurements of the local energy balance over a coral reef flat, Heron Island, southern Great Barrier Reef, Australia. *Journal of Geophysical Research*, *115*, D19124. https://doi.org/10.1029/2010JD014218

McJannet, D. L., Cook, F. J., McGloin, R. P., McGowan, H. A., Burn, S., & Sherman, B. S. (2013). Long-term energy flux measurements over an irrigation water storage using scintillometry. *Agricultural and Forest Meteorology*, *168*, 93–107. https://doi.org/10.1016/j.agrformet.2012.08.013

Michel, D., Philipona, R., Ruckstuhl, C., Vogt, R., & Vuilleumier, L. (2008). Performance and uncertainty of CNR1 net radiometers during a one-year field comparison. *Journal of Atmospheric and Oceanic Technology*, *25*(3), 442–451. https://doi.org/10.1175/2007JTECHA973.1

Mumby, P. J., Chisholm, J. R. M., Edwards, J. A., Andrefouet, S., & Jaubert, J. (2001). Cloudy weather may have saved Society Island reef corals during the 1998 ENSO event. *Marine Ecology Progress Series*, *222*, 209–216. https://doi.org/10.3354/meps222209

Nordbo, A., Launiainen, S., Mammarella, I., Lepparanta, M., Huotari, J., Ojala, A., & Vesala, T. (2011). Long-term energy flux measurements and energy balance over a small boreal lake using eddy covariance technique. *Journal of Geophysical Research*, *116*, D02119. https://doi.org/10.1029/2010JD014542

Oke, T. R. (1978). *Boundary layer climates*. London: Routledge. https://doi.org/10.4324/9780203407219

Pandolfi, J. M., Connolly, S. R., Marshall, D. J., & Cohen, A. L. (2011). Projecting coral reef futures under global warming and ocean acidification. *Science*, *333*(6041), 418–422. https://doi.org/10.1126/science.1204794

Phinn, S. R., Roelfsema, C., & Mumby, P. (2011). Multi-scale, object-based image analysis for mapping geomorphic and ecological zones on coral reefs. *International Journal of Remote Sensing*, *33*, 3768–3797.

Schmid, H. P. (1994). Source areas for scalars and scalar fluxes. *Boundary-Layer Meteorology*, *67*(3), 293–318. https://doi.org/10.1007/BF00713146

Schmid, H. P., Grimmond, C. S. B., Cropley, F., Offerle, B., & SuB, H.-B. (2000). Measurements of CO_2 and energy fluxes over a mixed hardwood forest in the mid-western United States. *Agricultural and Forest Meteorology*, *103*(4), 357–374. https://doi.org/10.1016/S0168-1923(00)00140-4

Smith, N. (2001). Weather and hydrographic conditions associated with coral bleaching: Lee Stocking Island, Bahamas. *Coral Reefs*, *20*(4), 415–422. https://doi.org/10.1007/s00338-001-0189-2

Swan, H. B., Crough, R. W., Vaattovaara, P., Jones, G. B., Deschaseaux, E. S. M., Eyre, B. D., et al. (2016). Dimethyl sulfide and other biogenic volatile organic compound emissions from branching coral and reef seawater: Potential sources of secondary aerosol over the Great Barrier Reef. *Journal of Atmospheric Chemistry*, *73*(3), 303–328. https://doi.org/10.1007/s10874-016-9327-7

Tanaka, H., Hiyama, T., & Nakamura, K. (2008). Turbulent flux observations at the tip of a narrow cape on Miyako Island in Japan's southwestern islands. *Journal of the Meteorological Society of Japan*, *86*(5), 649–667. https://doi.org/10.2151/jmsj.86.649

Tani, M., Yamamoto, S., Leclerc, M. Y., & Leuning, R. (2008). Special issue on Asiaflux—Foreword. *Agricultural and Forest Meteorology*, *148*(5), 697–699. https://doi.org/10.1016/j.agrformet.2008.01.002

Tenhunen, J. D., Valentini, R., Kostner, B., Zimmermann, R., & Granier, A. (1998). Variation in forest gas exchange at landscape to continental scales. *Annales des Sciences Forestières*, *55*(1-2), 1–11. https://doi.org/10.1051/forest:19980101

Theobald, A., McGowan, H., Speirs, J., & Callow, N. (2015). A synoptic classification of inflow-generating precipitation in the Snowy Mountains, Australia. *Journal of Applied Meteorology and Climatology*, *54*(8), 1713–1732. https://doi.org/10.1175/JAMC-D-14-0278.1

Tsukamoto, O., Ohtaki, E., Iwatani, Y., & Mitsuta, Y. (1991). Stability dependence of the drag and bulk transfer coefficients over a coastal sea surface. *Boundary-Layer Meteorology*, *57*, 359–375.

Vesala, T., Huotari, J., Rannik, U., Suni, T., Smolander, S., Sogachev, A., et al. (2006). Eddy covariance measurements of carbon exchange and latent and sensible heat fluxes over a boreal lake for a full open-water period. *Journal of Geophysical Research*, *111*, D11101. https://doi.org/10.1029/2005JD006365

Wanninkhof, R., Asher, W. E., Ho, D. T., Sweeney, C. S., & McGillis, W. R. (2009). Advances in quantifying air-sea gas exchange and environmental forcing. *Annual Review of Marine Science*, *1*(1), 213–244. https://doi.org/10.1146/annurev.marine.010908.163742

Webb, E. K., Pearman, G. I., & Leuning, R. (1980). Correction of flux measurements for density effects due to heat and water vapour transfer. *Quarterly Journal of the Royal Meteorological Society*, *106*(447), 85–100. https://doi.org/10.1002/qj.49710644707

Weibe, A., Sturman, A., & McGowan, H. (2011). Wavelet analysis of atmospheric turbulence over a coral reef flat. *Journal of Atmospheric and Oceanic Technology*, *28*(5), 698–708. https://doi.org/10.1175/2010JTECHA1485.1

Woodroffe, C. D. (2003). *Coasts: Form, process and evolution* (623 pp.). New York: Cambridge University Press.

Yan, H. Q., Yu, K. F., Shi, Q., Tan, Y. H., Zhang, H. L., Zhao, M. X., et al. (2011). Coral reef ecosystems in the South China Sea as a source of atmospheric CO_2 in summer. *Chinese Science Bulletin*, *56*(7), 676–684. https://doi.org/10.1007/s11434-011-4372-8

Yarnal, B. (1993). *Synoptic climatology in environmental analysis: A primer*. London: John Wiley and Sons. 256p

Yu, G. R., Wen, X. F., Sun, X. M., Tanner, B. D., Lee, X. H., & Chen, J. Y. (2006). Overview of ChinaFLUX and evaluation of its eddy covariance measurement. *Agricultural and Forest Meteorology*, *137*(3–4), 125–137. https://doi.org/10.1016/j.agrformet.2006.02.011